Rectification of El Nino-Southern Oscillation into Climate Anomalies of Decadal and Longer Time-Scales: Results From Forced Ocean GCM Experiments

De-Zheng Sun[1], Tao Zhang[1], Yan Sun[1, 2], and Yongqiang Yu[3]

[1] *Cooperative Institute for Research in Environmental Sciences, University of Colorado & NOAA/Earth System Research Laboratory/Physical Science Division, Boulder, Colorado*

[2] *Key Laboratory of Ocean Circulation and Waves, Institute of Oceanology, Chinese Academy of Sciences, Qingdao, China*

[3] LASG, Institute of Atmospheric Physics, Chinese Academy of Sciences, China

ABSTRACT

To better understand the causes of climate change in the tropical Pacific on the decadal and longer time scales, the rectification effect of ENSO events is delineated by contrasting the time-mean state of two forced ocean GCM experiments. In one of them, the long-term mean surface wind stress of 1950—2011 is applied while in the other, the surface wind stress used is the long-term mean surface wind stress of 1950-2011 plus the interannual monthly anomalies over the period. Thus the long-term means of the surface wind stress in the two runs are identical. The two experiments also use the same relaxation boundary conditions---the SST is restored to the same prescribed values. The two runs, however, are found to yield significantly different mean climate for the tropical Pacific. The mean state of the run with interannual fluctuations in the surface winds is found to have a cooler warm-pool, warmer thermocline water, and warmer eastern surface Pacific than the run without interannual fluctuations in the surface winds. The warming of the eastern Pacific has a pattern that resembles the observed decadal warming. In particular, the pattern features an off-equator maximum as the observed decadal warming. The spatial pattern of the time-mean upper ocean temperature differences between the two experiments is shown to resemble that of the differences in the nonlinear dynamic heating, underscoring the role of the nonlinear ocean dynamics in the rectification. The study strengthens the suggestion that rectification of ENSO can be a viable mechanism for climate change of decadal and longer time-scales.

1. Introduction

Among the many milestones marking the conceptual advances in our understanding of the original of natural climate variability, we find that the study by Kessler and Kleeman (2000) stands out as distinctly as that by Hasselmann (1976) in their originality of pointing out that climate variability of one time-scale can be an important cause or significant contributor for climate variability of a different time-scale. Specifically, the study by Kessler and Kleeman (2000) points out that the Madden-Julian Oscillation (MJO)--an intra-seasonal climate signal in the surface winds- can be converted to a Sea Surface Temperature (SST) anomaly in the tropical Pacific that resembles what is normally associated with El Nino Southern Oscillation (ENSO)—an inter-annual climate signal. The underlying mechanism for this conversion is provided by nonlinear ocean dynamics ("nonlinear rectification" in the words given by this study). A question that naturally follows up on the study of Kessler and Kleeman (2000) is whether this up-scale conversion stops with MJO and ENSO. Can ENSO signal in the surface winds be converted to SST anomalies resembling to the observed decadal signal—the tropical Pacific decadal variability (Zhang et al. 1997)? The present paper deals with this question in a manner that is analogous to that by Kessler and Kleeman (2000). This study is also meant to complement the earlier studies by some of the present authors using a hybrid coupled model (Sun and Zhang 2006, Sun 2007) as well as an analytical model (Liang et al. 2012) in delineating the time-mean effect of ENSO events.

The observational motivation for this study is provided by Fig. 1. The regime-like shift in the tropical SST since 1976 (Wang and Ropelewski 1995; Zhang et al. 1997) is accompanied with a change in the level of ENSO variability – the variance of the interannual variability of the tropical Pacific SST (Fig. 1b). The level of ENSO activity during the epoch with a warmer time-mean SST in the eastern tropical Pacific is anomalously higher than the previous epoch with a colder time-mean SST in the eastern tropical Pacific. Is the change in the level of ENSO activity caused by the change in the time-mean state, or the change in the time-mean state is a consequence of the change in the level of ENSO activity?

A numbers of studies have examined the impact of a warming in the mean state of the tropical Pacific on the level of ENSO activity (Fedorov and Philander 2000, 2001; An and Jin 2001; and Wang and An 2001 among others). These studies employ the traditional linear instability analysis of the mean state and deduce the impact of changes in the mean state on the growth rate of the ENSO modes. These studies have nicely illuminated a consistency between the changes in the level of ENSO activity and the corresponding changes in the time-mean state, within the mathematical framework of linear instability analysis. However, these studies do not address the cause of the warming in the time-mean state, in particular the question whether an increase in the level of ENSO activity can induce a warming in the time-mean state resembling the observed decadal warming (Fig. 1a).

The possibility that ENSO may have an important time-mean effect on the tropical Pacific climatology has been highlighted by studies of the role of ENSO events in the long-term heat balance of the tropical Pacific. Using a hybrid coupled model in which the ocean component is an upper ocean GCM—the NCAR Pacific basin model (Gent and Cane 1989) — a model that has an explicit heat budget for the subsurface ocean, Sun (2003) not only finds a positive impact of an increase in the tropical maximum

SST on the amplitude of ENSO, but also finds that in the presence of ENSO, the time-mean zonal SST contrast is less sensitive to an increase in the tropical maximum SST than in the absence of ENSO because the resulting stronger ENSO variations tend to cool the western Pacific and warm the eastern Pacific. The time-mean effect of ENSO events was further studied in Sun and Zhang (2006). In the experiments conducted in this study, they perturbed the long-term heat balance of the model in more variety ways including subjecting the model to an enhanced cooling in the subtropics as well as to an increase in the tropical heating. Again, they find that the response in the upper ocean temperature to an increase in the tropical heating is very different between the case with ENSO and the case without ENSO. The results suggest that the time-mean effect of ENSO events is to cool the western Pacific warm-pool, warm the subsurface thermocline water and the broad region of the surface tropical eastern Pacific (see Fig. 4 in that study). Sun (2007) discussed the implications of the time-mean effect of ENSO events for understanding the response of the tropical Pacific climate to the rise of CO_2 in the atmosphere.

There are also more empirically based studies of the time-mean effect of ENSO events (Rodger et al. 2004; Yeh and Kirtman 2004, Sun and Yu 2009; Yu and Kim 2011, Choi et al. 2011). These studies note the surface manifestation of the asymmetry between El Niño and La Niña events – the strongest El Niño event, measured by the Niño3 SST anomaly, being stronger than the strongest La Niña event – has long been noted (Zebiak and Cane 1987; Burgers and Stephenson 1999). Rodger et al. 2004 and Yeh and Kirtman 2004 are probably among the first to suggest that decadal variability in the tropical Pacific may result from a “residual” effect of ENSO on the background state due to the asymmetry between El Niño and La Niña events.

They find respectively in a long simulation by two different coupled GCMs that changes in the mean state between decades with high ENSO activity and decades with low ENSO activity resemble the residual of the two phases of ENSO in the model. They thereby suggest that the asymmetry could be a mechanism for decadal changes in the tropical Pacific SST. Noting a 15 year cycle in the level of ENSO activity in an extended SST data set consisting of historical and paleo-climate data, and a change in the asymmetry of ENSO with this decadal cycle, Sun and Yu (2009) have argued that the residual effect from the ENSO asymmetry may provide an explanation for the decadal cycle they have noted in the level of ENSO activity. A similar conclusion has been reached by examining a long-term simulation of GFDL coupled GCM CM2.1 (Choi et al. 2011). Yu and Kim (2011) have further investigated the decadal variability in CMIP3 models from the angle of ENSO asymmetry. Specific mechanisms have also been proposed to explain the asymmetry between the two phases of ENSO. Jin et al. (2003) and An and Jin (2004) suggest that the asymmetry is due to the nonlinear term in the heat budget equation for the surface ocean. Schopf and Burgman (2006) have showed that the skewness of the SST distribution could be due to a kinematic effect of oscillating a nonlinear temperature profile.

A basic assumption is implicit in these empirical studies: asymmetry results in a time-mean effect of ENSO events. ENSO asymmetry by itself does not guarantee a significant time-mean effect of ENSO events, however. The asymmetry between the two phases of ENSO only suggests a non-zero residual effect of ENSO, to the extent that a finite threshold value is used to define El Niño and La Niña events. But because such a residual effect will depend quantitatively on how you define El Niño and La Niña events, the asymmetry alone does not necessarily imply a significant time-mean (or rectification) effect of ENSO. For the same reason, while we may divide the observations and model simulations of ENSO into epochs with different levels of ENSO activity and then try to discern the time-mean effect of ENSO by contrasting the mean states of these epochs as done in Rodgers et al. (2004), we can only confirm through this approach a correspondence between a change in the level of ENSO activity and a change in the mean state. A correspondence between the degree of asymmetry of ENSO and its time-mean effect is found in a nonlinear box model for the tropical Pacific (Liang et al. 2012), but they show that this correspondence occurs not because the former causes the latter, but because they are both caused by the nonlinear term in the heat budget equation.

The approach employed by Liang et al. (2011) is novel in that they quantify the time-mean effect of ENSO by contrasting the equilibrium state of the coupled tropical ocean-atmosphere with the actual realized climatology. At the equilibrium, ENSO as an instability has not manifested while in the actual realized climatology ENSO has manifested. Thus, the difference between the two is a good measure of the ENSO effect in the climatology. Indeed, they have succeeded in doing such analysis with the use of an analytical model. The model is a highly simplified representation of the coupled tropical ocean-atmosphere system, but it encapsulates the major physics of the ENSO system. In the context of this model, they show unambiguously that the time-mean effect of ENSO is a warming to the eastern tropical Pacific. The simplicity of the model, however, does not give the corresponding meridional structure of the warming, limiting the application of the mechanism revealed in that model to the observed decadal warming. A key feature of the observed warming in the eastern tropical Pacific is the off-equatorial maximum in contrast to the El Nino warming or the residual SST signal between the two phase of ENSO. Nonetheless, the results of Liang et al. (2011) demonstrate the origin of the rectification—the nonlinear advection of heat by ocean currents, suggesting rectification effect may show up even in forced ocean GCM experiments.

In this paper, we explore the time-mean effect of ENSO events by conducting forced ocean GCM experiments. The methodology is analogous to that used by Kessler and Kleeman (2000) in their study of the rectification effect of MJO on ENSO. In the present study, the fluctuations in the surface wind stress are interannual fluctuations and the "rectified" effect of these fluctuations are climate anomalies on the decadal and longer time-scales. Complementing the study by Liang et al. (2012), the present methodology will allow us to see the meridional structure of the rectified warming to the eastern Pacific. A distinguished feature in the meridional structure of the observed tropical decadal warming in the eastern tropical Pacific is that the maximum warming is located off equator because of an apparent minimum warming right on the equator (Fig. 1a). This feature is in contrast to the residual between El Nino and La Nina which has its maximum right on the equator.

This remaining of paper is organized as follows. Methodology and the model used for the experiments are described in Section 2. Key results from this study are reported in Section 3. Some key implications from the results are provided in Section 4.

2. Methodology

As already mentioned, the methodology is similar to that of Kessler and Kleeman

(2000) except that it is applied to delineate the rectification effect of ENSO time-scale fluctuations onto the climate variability on the decadal and longer time-scales. Two experiments are conducted with a tropical upper ocean GCM. In one of them, the long-term mean surface wind stress of 1950—2011—the surface wind stress averaged over the entire period-- is applied (Eq. 1A), while in the other, the surface wind stress used is the long-term mean of 1950-2011plus the interannual monthly anomalies over the period (Eq. 1B),

$$\vec{\tau}_A = \vec{\tau}_o \tag{1A}$$

$$\vec{\tau}_B = <\vec{\tau}_o> + \vec{\tau}'_o \tag{1B}$$

where <> represents the long-term mean and $\vec{\tau}'_o$ is the interannual anomaly relative to the long-term mean,

$$\vec{\tau}'_o = \vec{\tau}_o - <\vec{\tau}_o> \tag{2}$$

Thus the long-term means of the surface wind stress in the two runs are identical as the anomalies are by design to have zero long-term mean,

$$<\vec{\tau}_A> = <\vec{\tau}_B> \tag{3}$$

The two experiments also use the same linear relaxation boundary condition---the SST is linearly restored to the same prescribed values,

$$F_s = cC_p\rho H_m(SST_p - SST) \tag{4}$$

where F_s is the net surface heat flux into the ocean, C_p is the specific heat, ρ is the density of water, c is the restoring coefficient, H_m is the depth of the mixed layer which has a fixed value in the ocean model (50 m), SST_p is the prescribed equilibrium SST, and SST is the actual model predicted SST. Eq. (4) is the same as Eq. (2) in Sun (2003). The form of SST_p used here is also the same as in Sun (2003)—it is constant with time and is zonally symmetric (see Eq. (5) in Sun (2003)).

If the ocean dynamics is linear, then the time-mean state of the two experiments should be identical.

The tropical upper ocean GCM used here is the NCAR Pacific basin model (Gent and Cane 1989, Gent 1991). The model has fine spatial resolution for the equatorial ocean ($1^{\mathbf{o}}$ by 0.25^{o}). It is the same tropical upper ocean model used by Kessler and Kleeman (2000) except a restoring thermal boundary condition (Eq. (4)) rather than using the original formulation by Seager et al. (1988). This allows us to focus on delineating the nonlinearity in the upper ocean dynamics. As we will see, the restoring boundary condition provides a realistic simulation of ENSO when forced with the observed windstress. The surface wind stress used for the pair of experiments is from NCEP (Kalnay et al 1996).

3. Results

3.1 ENSO in the forced ocean experiments

With ENSO fluctuations included in the surface wind forcing, the model simulates the ENSO events as manifested in the SST field as well as in the upper ocean temperatures. Fig. 2 compares the time series of the Nino3 SST from observations and the forced ocean GCM experiment. The simulation captures all the observed El Nino events. The two strongest events in the instrumental record—the 1982-83 El Nino and the 1997-98 El Nino event are well simulated in both timing and magnitude. The overall correlation between the simulated monthly Nino3 anomalies and those in the observations are about 0.75. The composite of the warm phase and cold phase SST anomalies are shown in Fig.3 together with their residuals (warm phase + cold phase) as a measure of the ENSO asymmetry in the surface field. A 0.5 ^{o}C threshold value for the monthly SST anomaly was used for obtaining the warm phase and cold phase composites and the same criterion was used for both the model data and observations. The major features of the spatial pattern of the SST anomalies in both of the two phases are well simulated. The only noticeable discrepancy with the observations is found in the immediate region of the coast, particularly in the cold phase. The SST anomaly for the cold phase in the observations has its maximum clearly detached from the coast, but this feature is less distinct in the model simulations. The consequence on the asymmetry pattern is that ENSO in the models is slightly less asymmetric in the models than in the observations in the immediate region of the coast. But the overall pattern of the asymmetry is captured by the model, implying the nonlinear aspects of the dynamics are adequately represented in the model used.

The corresponding subsurface signatures from the observations and the model are further presented in Fig. 4. Again, the major features of the subsurface temperature anomalies for the two phases of ENSO are well captured by the models. The differences are quantitative and in the details. The most noticeable differences are an underestimate of the cooling to the western Pacific subsurface in the warm phase of ENSO, which in turn causes an underestimate of the cooling in the residual anomaly between the two phases. The warming in the eastern Pacific near the surface is less pronounced than in the observations during the warm phase of ENSO. The somewhat weaker El Nino evens as shown in the composite could be mostly due to the known biases in the NCEP wind-stress used (Guillermo et al. 2001, Wittenberg 2004). Overall and as far as the major features are concerned, ENSO events in the simulation are realistic and this gives confidence on the fidelity of the upper ocean dynamics as represented in the NCAR Pacific basin model.

3.2 Differences in the mean state between the two experiments

Despite the identical long-term surface wind stress and the identical restoring SST and restoring coefficient, the long-term mean climate is significantly different between the two forcing experiments. Fig. 5ab present the differences in the time-mean state of these two experiments measured respectively by the equatorial upper ocean temperature (Fig. 5a) and the SST (Fig.5b). The difference is characterized by a cooling of the western Pacific warm-pool, a warming of the equatorial thermocline water, a warming of the central equatorial Pacific, and a warming of the broad region of the surface eastern tropical Pacific. Note that right on the equator in the far eastern Pacific, the climate with ENSO actually is somewhat cooler than in the one without ENSO, but the surrounding off-equatorial region is considerably warmer.

To gain a more quantitative understanding of the time-mean effect of ENSO events as a function of the variance of interannual fluctuations, we have done an additional forced ocean GCM experiment in which the magnitude of wind stress anomalies is amplified by 50%--the time series of the wind-stress anomalies is multiplied by 1.5. The magnitude of ENSO, as measured by the standard variation in the Nino3 SST is found to be increased about the same amount (i.e., 50%). The resulting differences in the time-mean upper ocean temperature and SST between the enhanced ENSO run and the control run without ENSO are presented in Fig.6ab. Comparing Fig.6ab with their counterparts in Fig. 5, we see that the time-mean effect of ENSO is further enhanced as the variance of ENSO in the surface winds is further increased.

The time-mean effect of ENSO events as outlined by these differences between the two forced experiments are qualitatively consistent with what is found in Sun and Zhang (2006) (see their Fig. 4). The time-mean effect of ENSO as indicated by the present experiments are also consistent with those between the time-mean state and the equilibrium *state* found by Liang et al. (2011). Recall that they have found that in the presence of ENSO, the depth of the thermocline in the east is deeper in the time-mean state than in the equilibrium state. The reverse is true for the thermocline in the west. As the amplitude of ENSO increases, the depth of the thermocline in the time-mean state in the east Pacific becomes increasingly deeper than that in the equilibrium state, underscoring the impact of ENSO on the depth of the thermocline. Owing to a much more realistic ocean model, the present study reveals new features, in particular, the meridional structure of the warming in the tropical eastern Pacific as well as the pronounced cooling in the western Pacific.

3.3 Mechanisms responsible for the rectification

One key insight from the study of Liang et al. (2011) is that it is the nonlinear advection of heat in the upper ocean that is responsible for the rectification. In an earlier study by Jin et al (2002) focusing on the surface heat budget, they have also argued for the importance of the nonlinear dynamical heating (NDH) in the ENSO asymmetry and by implication the importance of this quantity for the corresponding rectified effect of ENSO into the mean state. Accordingly, we have calculated the NDH—the convergence of $\overline{V'T'}$ (where V' and T' are respectively the fluctuating part of the velocity and temperature relative to the long-term mean, and the over-bar denotes the time-average over 1950-2011 which covers many cycles of ENSO).

The distribution of NDH in the equatorial upper ocean (5^{o}S-5^{o}N) in the run with ENSO is presented in Fig. 7a. The pattern has a clear correspondence with that in the temperature differences between the run with ENSO and the run without ENSO in the surface forcing (Fig. 5a)—regions with a positive temperature difference in Fig.5a have heating in Fig. 7a while regions with a negative temperature difference in Fig5a have a cooling in Fig.7a. The distribution of NDH in the surface layer of the tropical Pacific is shown in Fig. 7b. The pattern also resembles that in Fig.5b closely with the exception for the region right on the equator in the eastern Pacific. In the heating pattern, it is warming right on the equator in the eastern Pacific, while in the temperature difference pattern, it is negative and therefore implies cooling. It turns out that this difference is due to the presence of NDH in the run without ENSO due to tropical instability waves (Legeckis 1977; Weisberg and Weingartner 1988; Qiao and Weisberg 1995; Qiao and Weisberg 1998). Recall that the ocean has fine spatial resolution for the equatorial region (1^{o} by 0.25^{o}) and is able to resolve tropical instability waves (Gent and Cane 1989, Gent 1991). When the NDH presented in the run with climatological winds is deducted from the NDH in the run with ENSO forcing (Fig. 8b), the region right on the equator again has negative heating in that region, consistent with the sign of the time-mean temperature difference in that region. It has been shown before that instability waves contribute significantly to the heating of the equatorial cold-tongue (Jochum and Murtugudde 2004; Menkes et al. 2006; Seo et al. 2006, An 2008). In particular, An (2008) has shown that that the heating to the equatorial cold-tongue from the instability waves has a nonlinear relationship with the intensity of the cold-tongue, resulting a residual effect when ENSO is presented. The present results (Fig. 7b and Fig. 8b) are consistent with the finding of An (2008). Thus, the equatorial minimum of the time-mean effect of ENSO in the eastern tropical Pacific appears to have a lineage with the asymmetric dynamics of the instability waves, underscoring the depth of dependence of climate anomalies of a longer time-scale on climate processes of shorter time-scales.

The overall pattern of NDH shown in Fig. 7 and Fig. 8 is mainly determined from its zonal component—the advection of the anomalous temperature by the anomalous zonal current. Fig. 9 and Fig. 10 present the three components of the total NDH shown in Fig. 7 and Fig. 8 respectively. Note that the close resemblance between the zonal component of the NDH and the total NDH. In terms of magnitude, the meridional component and the vertical component of NDH are as significant as the zonal component, but their broad spatial pattern is different from that of the total NDH. In fact, the meridonal component and the vertical component largely cancel each other in the equatorial upper ocean except in the surface layer. Focusing on the warming in the surface eastern Pacific however, the meridional component of the NDH is also a significant contributor (Fig. 10).

4. Implications

The study advances our understanding of the time-mean effect of ENSO events on the thermal structure of the equatorial upper Pacific ocean beyond that from the empirical studies (Rodger et al. 2004; Yeh and Kirtman 2004, Schopf and Burgman 2006, Sun and Yu 2009, Yu and Kim 2011). In particular, it shows that using the residuals between the two phases of ENSO to represent the time-mean effect of ENSO is only good for the broad pattern of the effect, but inaccurate in details. The differences are particularly noteworthy in the equatorial eastern Pacific--the residual SST anomaly between the two phases of ENSO in the eastern Pacific has its maximum right on the equator, but the rectified effect of ENSO events obtained by the present method has an off-equator maximum.

The newly identified feature in the spatial pattern of the rectified effect of ENSO events in the eastern Pacific-- the off-equator maximum, however, is in the observed decadal warming in the eastern Pacific (Fig.1a). Thus the present results actually add weight to the argument that the recent decadal warming in the eastern tropical Pacific may be a consequence of the elevation of ENSO events during this period, and more generally to the suggestion that a nonlinear interaction between ENSO events and the time-mean state may act as a viable mechanism for decadal variability in the tropical Pacific region. Specifically, the present results combined with the studies by Fedorov and Phliander (2000, 2001) and Liang et al. (2012) allow us to envision the following scenario as a possible explanation for decadal variability in the tropical Pacific: an initial increase in the level of ENSO activity results in a warming in the eastern Pacific which in turn enhances the increase in the level of ENSO activity. (Recall that a decadal warming in the background state can cause an elevation of ENSO activity (Fedorov and Philander 2000, 2001; An and Jin 2001; and Wang and An 2001)). As the associated deepening of the thermocline in the eastern Pacific exceeds a critical value, the reduced thermocline feedback is no longer able to sustain the level of ENSO activity already achieved, and the level of the ENSO activity then starts to decline (Fedorov and Philander 2000, 2001). The decline in the level of ENSO activity allows the radiative forcing that has been working in the background to retake preeminence to bring the system closer to its equilibrium—an unstable situation that is characterized by a larger thermal contrast between the warm-pool water and the thermocline water (Liang et al. 2010). This unstable situation reopens the stage for another strong epoch of ENSO activity. The relevance of this picture to the decadal variability in the real world and in the models will be explored in detail in a subsequent paper. Tree-ring records analyzed by Li et al. (2011) indicate that interdecadal modulation of ENSO amplitude and its close coupling with interdecadal tropical Pacific mean climate change had been a norm in the past millennium. An analysis of the tropical Pacific decadal variability in a 2000-year integration with the Geophysical Fluid Dynamics Laboratory Climate (Delworth et al. 2006, Wittenberg 2009) from the rectification prospective suggests that the rectification effect of ENSO time-scale variability is involved in the tropical Pacific decadal variability generated by the model (Ogata et al. 2012). An analysis of the variability on centennial time-scales in the same model also reveals a spatial pattern of the variability resembling the time-mean effect of ENSO as revealed here (Karnauskas et al. 2012), raising the prospective that the importance of the rectification effect of ENSO may not be limited to variability on decadal time-scales. Indeed, proxy data for the tropics indicate that the medieval climate anomaly (MCA) and the little ice age (LIA) were accompanied significant changes in the level of ENSO activity (Rein et al 2004, Cobb et al. 2003, Graham et al. 2007).

The present results also show more clearly that the rectified effect of ENSO has a complex spatial structure in the equatorial upper ocean (Fig. 5 and Fig. 6): an overall reduction in the thermal contrast between the surface warm-pool and the subsurface thermocline water is accompanied by a strengthening of the vertical stratification in the central equatorial Pacific. Thus the present study may also potentially provide a path to understand the dynamics behind the suggestion from empirical studies that the transition (or change) from a weak ENSO regime to a strong ENSO regime (or vice versa) on decadal and longer time-scales may be accompanied by a change in the dominance by the two types of El Nino events--the central Pacific El Nino (warm-pool El Nino or Modoki) and the eastern Pacific El Nino) (Sun and Yu 2009, Yeh et al. 2009, Lee and McPhaden 2010, McPhaden et al. 2011). Will the initial stabilization to the far eastern Pacific from an increase in the variance of ENSO be necessarily accompanied by a destabilization of the central Pacific? Will the eventual turn-around of the decadal warming follow right after the stabilization of the central Pacific region is completed? Those issues are clearly interesting and will be addressed in a subsequent study.

The current finding also highlights that the time-mean effect of ENSO includes a substantial cooling to the warm-pool. The cooling is much more profound, particularly at the surface level than the traditional ENSO residual map had suggested. The present finding of a profound cooling to the western Pacific by the collective effect of El Nino events highlights a role for other factors in causing the observed warming in the western Pacific over the last few decades. Recall that in the two experiments conducted in the present study, the thermal boundary conditions are kept identical in order to isolate the role of upper ocean dynamics in rectifying ENSO. To fully investigate the causes of the change in the tropical Pacific SST, one has to consider the increase in the tropical maximum SST due to enhanced radiative heating or other possible factors other than the nonlinear effect from ENSO dynamics. Based on a coupled model, Sun (2003) has suggested that the elevated ENSO activity during recent decades may be a consequence of the increasing tropical maximum SST. Combing the results of Sun (2003) and the present results, the following scenario surfaces as an enticing explanation for what has been going on over the last few decades in the tropical Pacific: owning to a deterministic external heating (such as the rise of CO_2) or accumulated effect from weather events, the SST in the center of the warm-pool (the tropical maximum SST) has been experiencing a rise. In response, ENSO activity increases (Sun 2003), which results in a broad decadal warming signal in the central and eastern Pacific, but the corresponding cooling to the western Pacific is not strong enough to offset the decadal rise in the SST over that region forced by the external forcing or by the accumulated effect from the random weather events. This also means that without the time-mean effect of ENSO events, we would have seen a more pronounced warming in the warmest part of the world's open oceans. Whether this scenario can be an adequate explanation for what has been happening over the last few decades in the tropical Pacific will be investigated in a subsequent study that will take into account the increases in the radiative heating due to the rise of CO2 as well as the Hasselmann effect on the warm-pool SST from the weather events.

ACKNOWLEDGEMENTS

This research was supported by a grant from NSF Climate and Large-Scale Dynamics Program (AGS 0852329) and by grants from NOAA office of global programs--the Earth System Science Program (ESS) and the Modeling, Analysis, and Prediction Program (MAPP). The leading author would like to thank Dr. Mark Cane, Dr. Fei-Fei Jin, Dr. Michael McPhaden, and Dr. Richard Seager for their encouragements on this line of work on ENSO.

REFERENCE

An, S.-I., 2008: Interannual Variations of the Tropical Ocean Instability Wave and ENSO. *J. Climate*, **21**, 3680–3686.

An, S.-I., and F.-F. Jin, 2001: Collective role of thermocline and zonal advective feedbacks in the ENSO mode. *J. Climate*, **14,** 3421-3432.

An, S.-I., and F.-F., 2004: Nonlinearity and asymmetry of ENSO. *J. Climate*, **17,** 2399-2412.

An, S.-I., Y.-G. Ham, J.-S.Kug, F.-F. Jin, and I.-S. Kang, 2005: El Niño - La Niña asymmetry in the coupled model intercomparison project simulations. *J. Climate*, **18,** 2617-2627.

Burgers, G., and D. B. Stephenson, 1999: The "normality" of El Niño. *Geophys. Res. Lett.*, **26,** 1027-1030, doi:10.1029/1999GL900161.

Cane, M.A., 2010: Decadal Predictions in Demand. *Nature Geoscience*, Advance online publication, pp. 231-232.

Choi, J., S.-I. An, and S.W. Yeh, 2011: Decadal amplitude modulation of two types of ENSO and its relationship with the mean state. *Climate Dynamics,* **38**, 2631-2644.

Cobb, K.M., C.D. Charles, H. Cheng, and R. L. Edwards, 2003: El Nino/Southern Oscillation and tropical Pacific climate during the last millennium. *Nature*, **424,** 271-276.

Collins, M., and Coauthors, 2010: The impact of global warming on the tropical Pacific ocean and El Niño. *Nat. Geosci.*, **3,** 391-397.

Delworth, T. L., et al. (2006), GFDL's CM2 global coupled climate models. Part I: Formulation and simulation characteristics, *J. Climate*, **19**, 643–674.

Fedorov, A. V., and S. G. Philander, 2000: Is El Niño changing? *Science*, **288,** 1997-2002.

Fedorov, A. V., and S.G. Philander, 2001: A stability analysis of tropical ocean-atmosphere interactions: Bridging measurements and theory for El Niño. *J. Climate*, **14**, 3086-3101.

Guilyardi, E., A. Wittenberg, A. Fedorov, M. Collins, C. Wang, A. Capotondi, G. J. van Oldenborgh, and T. Stockdale, 2009: Understanding El Niño in ocean-atmosphere general circulation models. *Bull. Amer. Meteor. Soc.*, **90,** 325-340.

Guilyardi, W. J. Cai, M. Collins, A. Fedorov, F.-F. Jin, A. Kumar, D.-Z. Sun, A. Wittenberg, 2011: New strategies for evaluating ENSO processes in climate models. *Bull. Amer. Meteor. Soc* ., **236,** 235-238.

Gent, P. R., 1991: The heat budget of the TOGA-COARE domain in an ocean model. J. Geophys. Res., 96, 3323–3330.

Gent, P. R., and M. A. Cane, 1989: A reduced gravity, primitive equation model of the upper equatorial ocean. *Comp. Phys.*, **81**, 444-480.

Graham, N.E., M.K. Hughes, C.M. Ammann, K.M. Cobb, M.P. Hoerling, D.J. Kennett, J. P. Kennett, B. Rein, Lowell. Stott, P.E. Wigand, T. Xu, 2007: Tropical Pacific—Mid-latitude Teleconnections in Medieval times. *Climate Dynamics*, **83**, 241-285.

Guillermo, A., A. Miller, J.O. Roads, and D, Cayan, 2001: Pacific Ocean Wind Stress and Surface Heat Flux Anomalies from NCEP Reanalysis and Observations: Cross-statistics and Ocean Model Responses. *J. Geophys.*, **106**, 22249-22265.

Hasselmann, K. 1976: Stochastic Climate Models. *Tellus*, **28**, 473, 485.

Jin, F.-F., S.-I. An, A. Timmermann, and J. X. Zhao, 2003: Strong El Niño events and nonlinear dynamical heating. *Geophys. Res. Lett.*, **30,** 1120, doi:10.1029/2002GL016356.

Kalnay, E., and Coauthors, 1996: The NCEP/NCAR 40-Year Reanalysis Project. *Bull. Amer. Meteor. Soc.*, **77**, 437–471.

Karnauskas, K.B., J.E. Smerdon, R. Seager, and J.F. Gonzalez–Rouco, 2012: A Pacific Centennial Oscillation Predicted by Coupled GCMs. J. Climate, 25(17), 5943–5961.

Kessler, W.S. and R. Kleeman, 2000: Rectification of the Madden-Julian Oscillation into the ENSO cycle. *J. Climate,* **19**, 643–674.

Legeckis, R., 1977: Long waves in the eastern equatorial Pacific Ocean: A view from a geostationary satellite. *Science*, **197,** 1179–1181.

Li, J., S.-P. Xie, E. R. Cook, G. Huang, R. D'Arrigo, 544 F. Liu, J. Ma and X. Zheng, 2011: Interdecadal modulation of El Nino amplitude during the past millennium. Nature Climate Change, 1, 114-118.

Lee, T., and M. McPhaden, 2010: Increasing intensity of El Niño in the central-equatorial Pacific. Geophys. Res. Lett., **37**, L14603, 5 PP., doi:10.1029/2010GL044007.

Liang,J., Xiu-Qun Yang, and De-Zheng Sun, 2012: The effect of ENSO events on the Tropical Pacific Mean Climate: Insights from an Analytical Model. J. Climate, 25 , 7590-7606.

Meehl, G. A., A. Hu, C. Tebaldi, 2010: Decadal prediction in the Pacific region. *J. Climate*, **23**, 2959-2973.

Menkes, Christophe E. R., Jérôme G. Vialard, Sean C. Kennan, Jean-Philippe Boulanger, Gurvan V. Madec, 2006: A Modeling Study of the Impact of Tropical Instability Waves on the Heat Budget of the Eastern Equatorial Pacific. *J. Physical Oceanography,* **36**, 847–865.

Murtugudde, J., 2004, Internal variability in the tropical Pacific ocean. *Geophys. Res. Lett.*, **31**. Doi: 10.1029/2004GL02048.

Ogata, T., S.-P. Xie, A. Wittenberg, and D.-Z. Sun, 2012: Interdecadal amplitude modulation of El Nino/Southern Oscillation and its impacts on tropical Pacific decadal variability. *J. Climate*, accepted.

Qiao, L., and R. H. Weisberg, 1995: Tropical instability wave kinematics: Observation from the Tropical Instability Wave Experiment. *J. Geophys. Res.*, **100,** 8677–8693.

Qiao, L., and R. H. Weisberg, 1998: Tropical instability wave energetics: Observations from the Tropical Instability Wave Experiment. *J. Phys. Oceanogr.*, **28,** 345–360

Philander, S. G., 1990: *El Niño, La Niña, and the Southern Oscillation.* Academic Press, 293 pp.

Picaut, J., F. Masia and Y. du Penhoat, 1997: An advective-reflective conceptual model for the oscillatory nature of the ENSO. *Science,* **277,** 663-666.

Rein, B., A. Lückge, and F. Sirocko, 2004: A major Holocene ENSO anomaly during the Medieval period, *Geophys. Res. Lett.,* **31**, L17211, doi:10.1029/2004GL020161.

Rayner, N. A., E. B. Horton, D. E. Parker, C. K. Folland, and R. B. Hackett, 1996: Version 2.2 of the Global sea-ice and Sea Surface Temperature data set, 1903-1994. September 1996, Climate Research, Technical Note 74 (CRTN74), Hadley Centre for Climate Prediction and Research, Meteorological Office, London Road, Bracknell, Berkshire RG12 2SY.

Rodgers, K. B., P. Friederichs, and M. Latif, 2004: Tropical Pacific decadal variability and its relation to decadal modulations of ENSO. *J. Climate*, **17,** 3761-3774.

Schopf, P. S., and R. J. Burgman, 2006: A simple mechanism for ENSO residuals and asymmetry. *J. Climate*, **19,** 3167-3179.

Seager, R., S. E. Zebiak and M. A. Cane, 1988: A Model of the Tropical Pacific Sea-Surface Temperature Climatology. *Journal of Geophysical Research-Oceans*, **93**(C2): 1265-1280.

Seo, H., M. Jochum, R. Murtugudde, and A. J. Miller, 2006: Effect of ocean mesoscale variability on the mean state of tropical Atlantic climate. *Geophys. Res. Lett.*, **33.**L09606, doi:10.1029/2005GL025651

Sun, D.-Z., 1997: El Niño: A coupled response to radiative heating? *Geophys. Res. Lett*, **24,** 2031-2034, doi:10.1029/97GL01960.

Sun, D.-Z., 2000: Global climate change and ENSO: A theoretical framework. *El Niño: Historical and Paleoclimatic Aspects of the Southern Oscillation, Multiscale variability and Global and Regional Impacts*, H. F. Diaz and V. Markgraf, Eds., Cambridge University Press, 443-463.

Sun, D.-Z., 2003: A possible effect of an increase in the warm - pool SST on the magnitude of El Niño warming. *J. Climate*, **16,** 185-205.

Sun, D.-Z., 2007: The Role of ENSO in Regulating its Background State. In "Nonlinear Dynamics in Geosciences", pages 537-555, Springer New York, 604 pages, Edited by J. Elsner and A. Tsonis.

Sun, D.-Z., 2010: The diabatic and nonlinear aspects of El Niño - Southern Oscillation: Implications for its past and future behavior, in *AGU Geophysical Monograph "Climate Dynamics: Why Does Climate Vary?"*, edited by D.-Z. Sun. and F. Bryan, pp.79-104, AGU, Washington, D. C.

Sun, D.-Z., and T. Zhang, 2006: A regulatory effect of ENSO on the time - mean thermal stratification of the equatorial upper ocean. *Geophys. Res. Lett.*, **33,** L07710, doi:10.1029/2005GL025296.

Sun, D.-Z., T. Zhang, C. Covey, S. A. Klein, W. D. Collins, J. J. Hack, J. T. Kiehl, G.A. Meehl, I. M. Held, and M. Suarez, 2006: Radiative and dynamical feedbacks over the equatorial cold-tongue: results from nine atmospheric GCMs. *J. Climate*, **19,** 4059-4074.

Sun, D.-Z., and Z. Liu, 1996: Dynamic ocean-atmosphere coupling: a thermostat for the tropics. *Science*, **272,** 1148-1150.

Sun, F. P., J.-Y. Yu, 2009: A 10-15-yr modulation cycle of ENSO intensity. *J. Climate*, **22,** 1718-1735.

Timmermann, A., and F.-F. Jin, 2002: A nonlinear mechanism for decadal El Niño amplitude changes. *Geophys. Res. Lett.*, **29,** 1003, doi:10.1029/2001GL013369.

Vecchi, G. A., A. Clement, and B. J. Soden, 2008: Examining the tropical Pacific's response to global warming. *Eos, Trans. Amer. Geophys. Union,* **89** (9), 81-83.

Wang, B., and S.-I. An, 2001: Why the properties of El Niño changed during the late 1970s. *Geophys. Res. Lett.*, **28,** 3709-3712.

Wang, X. L., and C.-F. Ropelewski, 1995: An assessment of ENSO-scale secular variability. *J. Climate*, **8,** 1584-1589.

Weisberg, R. H., and T. J. Weingartner, 1988: Instability waves in the equatorial Atlantic Ocean. *J. Phys. Oceanogr.*, **18,** 1641–1657.

Wittenberg, A. T., 2009: Are historical records sufficient to constrain ENSO simulations? *Geophys. Res. Lett.*, **36,** L12702, doi:10.1029/2009GL038710.

Wittenberg, A. T., 2004: Extended Wind Stress Analyses for ENSO. *J. Climate*, **17**, 2526–2540.

Yeh, S.-W. and B. P. Kirtman 2004: Tropical Pacific decadal variability and ENSO amplitude modulation in a CGCM. *J. of Geophys. Res.-Oceans*, **109**. DOI: 10.1029/2004GL021731

Yeh, S.-W., J.-S. Kug, B. Dewitte, M.-H. Kwon, B. Kirtman, and F.-F. Jin , 2009: El Niño in a changing climate, *Nature*, **461**, 511–514, doi:10.1038/nature08316.

Yu, J.-Y. and S. T. Kim, 2011: Reversed Spatial Asymmetries between El Nino and La Nina and their Linkage to Decadal ENSO Modulation in CMIP3 Models*, J. of Climate,* **24**, 5423-5434.

Zebiak, S. E., and M. A. Cane, 1987: A model El Niño - Southern Oscillation. *Mon Weather Rev*, **115,** 2262-2278.

Zhang, T., D.-Z. Sun, R. Neale, and P. J. Rasch, 2009: An evaluation of ENSO asymmetry in the Community Climate System Models: A view from the subsurface. *J. Climate*, **22**, 5933–5961.

Zhang, Y., J. M. Wallace, and D. S. Battisti, 1997: ENSO-like interdecadal variability: 1900-93. *J. Climate*, **10,** 1004-1020.

Figure Captions:

FIG. 1. (a) Sea Surface Temperature (SST) differences between two epochs: 1977–2003 and 1950–1976. (b) Niño3 SST time series. Niño3 SST (anomalies) (in color). The black solid line is the variance of Niño3 SST anomalies obtained by sliding a moving window of a width of 16 years. Note the epoch 1977–2003 has higher level of ENSO activity than the previous period 1950–1976. (SST data used are from the Hadley Center for Climate Prediction and Research) (Rayner et al. 1996).

FIG. 2. Time series of Nino3 SST anomalies from the forced ocean GCM experiment (dashed-line) and observations (solid line). The two time series have a correlation of 0.75 with each other and a standard deviation of 0.79 ^{o}C (simulation) and 0.86 ^{o}C (observation) respectively.

FIG. 3. ENSO SST anomalies—warm phase (a), cold phase (b), and residual (warm phase + cold phase) (c) in the observations (left panels) and in the forced ocean GCM experiment (right panels). A 0.5 ^{o}C threshold value for the monthly SST anomaly was used for obtaining the warm phase and cold phase composites. The same threshold value was used for both the model simulations and the observations.

FIG. 4: ENSO temperature anomalies in the equatorial upper ocean (5^{o}S-5^{o}N)--warm phase (a), cold phase (b), and residual (warm phase + cold phase) (d) from observations (left panels) and from the forced ocean GCM

experiment (right panels).). A 0.5 ^{o}C threshold value for the monthly SST anomaly was used for obtaining the warm phase and cold phase composites. The same threshold value was used for both the model simulations and the observations.

FIG. 5. (a) Time-mean temperature differences in the equatorial upper ocean (5^{o}S-5^{o}N) between the run with ENSO in the surface forcing and the run without ENSO in the surface forcing. (b) The corresponding SST differences.

FIG. 6. Same as in Fig. 5 except the ENSO fluctuations in the surface forcing of the forced run is enhanced by 50% (measured by standard deviation). The standard deviation of the resulting Nino3 SST with the enhanced ENSO fluctuations in the surface forcing is enhanced by about the same amount (from 0.79 ^{o}C to 1.15 ^{o}C).

FIG. 7. Distribution of Nonlinear Dynamics Heating (NDH) in the run with ENSO for the equatorial upper ocean (5^{o}S-5^{o}N) as a function of longitude and depth (a) and for the surface layer of the tropical Pacific as a function of latitude and longitude (b). The contours are the corresponding time mean upper ocean temperature (a) and SST (b).

FIG. 8. Same as in Fig. 7 except that they are the differences between the run with ENSO and the run without ENSO.

FIG. 9: The zonal (a), meridional (b), and vertical (c) components of the Nonlinear Dynamics Heating (NDH) in the equatorial upper ocean (5^{o}S-5^{o}N) as a function

of longitude and depth in the run with ENSO (left three panels). (Contours in these figures (a, b, c) are the corresponding time-mean upper ocean temperature). The right three panels (d, e, f) show respectively the same quantities as in left three panels, but with the corresponding term in the run without ENSO removed. (Contours in the figures (d, e, f) are the differences in the time-mean upper ocean temperature between the run with ENSO and the run without ENSO).

FIG. 10: The zonal (a), meridional (b), and vertical (c) components of the Nonlinear Dynamics Heating (NDH) as a function of longitude and latitude for the surface layer in the run with ENSO (left three panels). Contours in the figures (a, b, c) are the corresponding time-mean SST). The right three panels (d, e, f) show respectively the same quantity as in the left three panels, but with the corresponding term in the run without ENSO removed. (Contours in the figures (d, e, f) are the differences in the time-mean SST between the run with ENSO and the run without ENSO.)

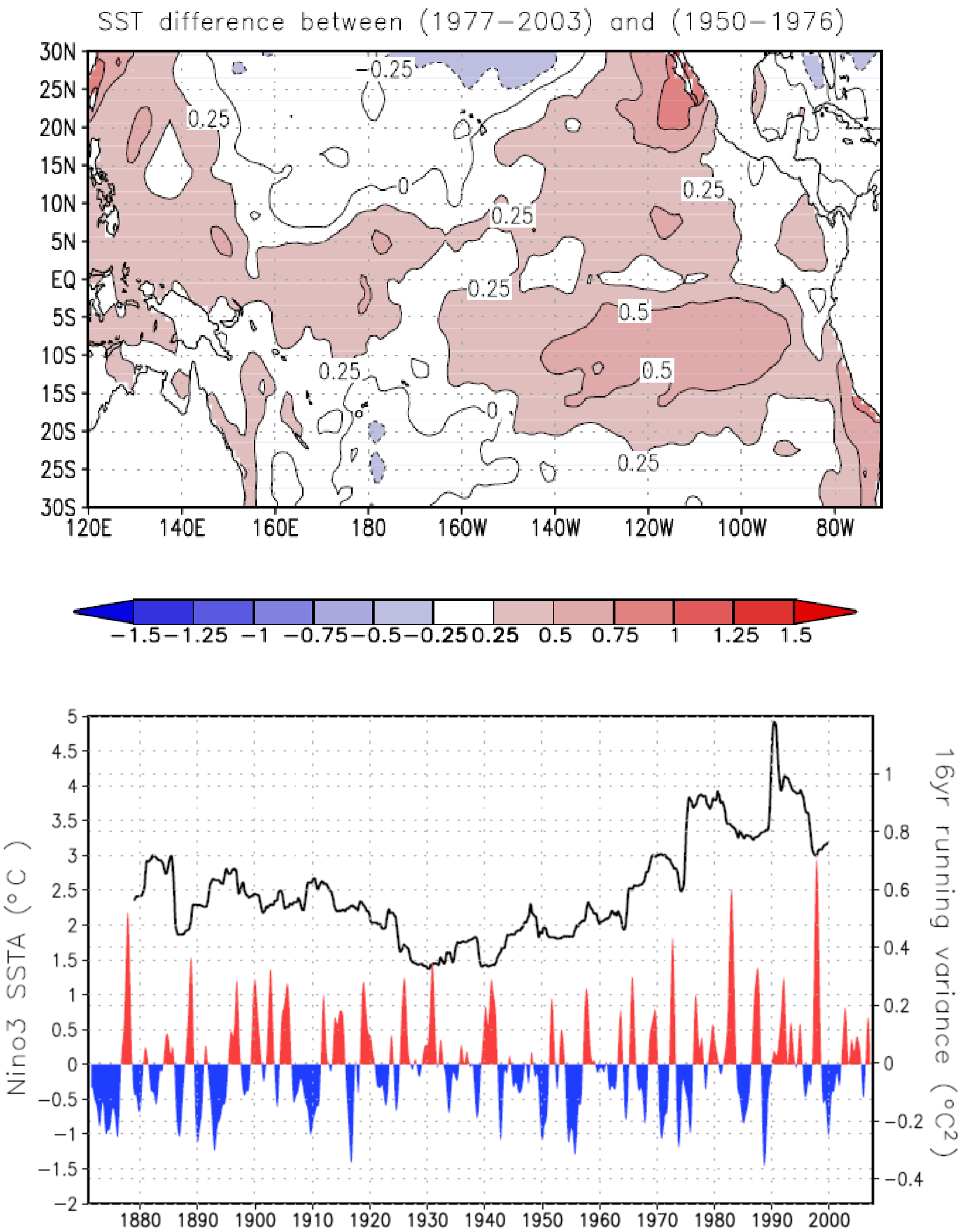

FIG. 1. (a) Sea Surface Temperature (SST) differences between two epochs: 1977–2003 and 1950–1976. (b) Niño3 SST time series. Niño3 SST (anomalies) (in color). The black solid line is the variance of Niño3 SST anomalies obtained by sliding a moving window of a width of 16 years. Note the epoch 1977–2003 has higher level of ENSO activity than the previous period 1950–1976. (SST data used are from the Hadley Center for Climate Prediction and Research) (Rayner et al. 1996).

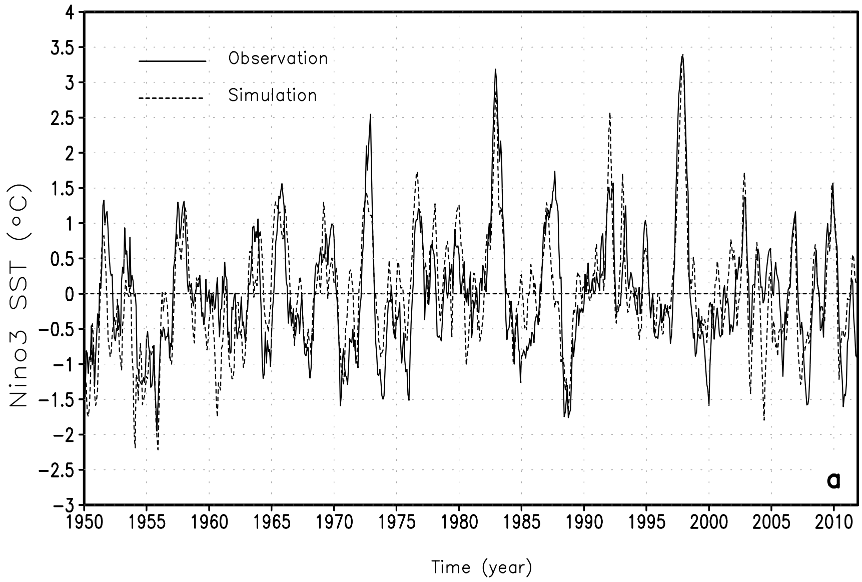

FIG. 2. Time series of Nino3 SST anomalies from the forced ocean GCM experiment (dashed-line) and observations (solid line) (Rayner et al. 1996). The two time series have a correlation of 0.75 with each other and a standard deviation of 0.79 ^{o}C (simulation) and 0.86 ^{o}C (observation) respectively.

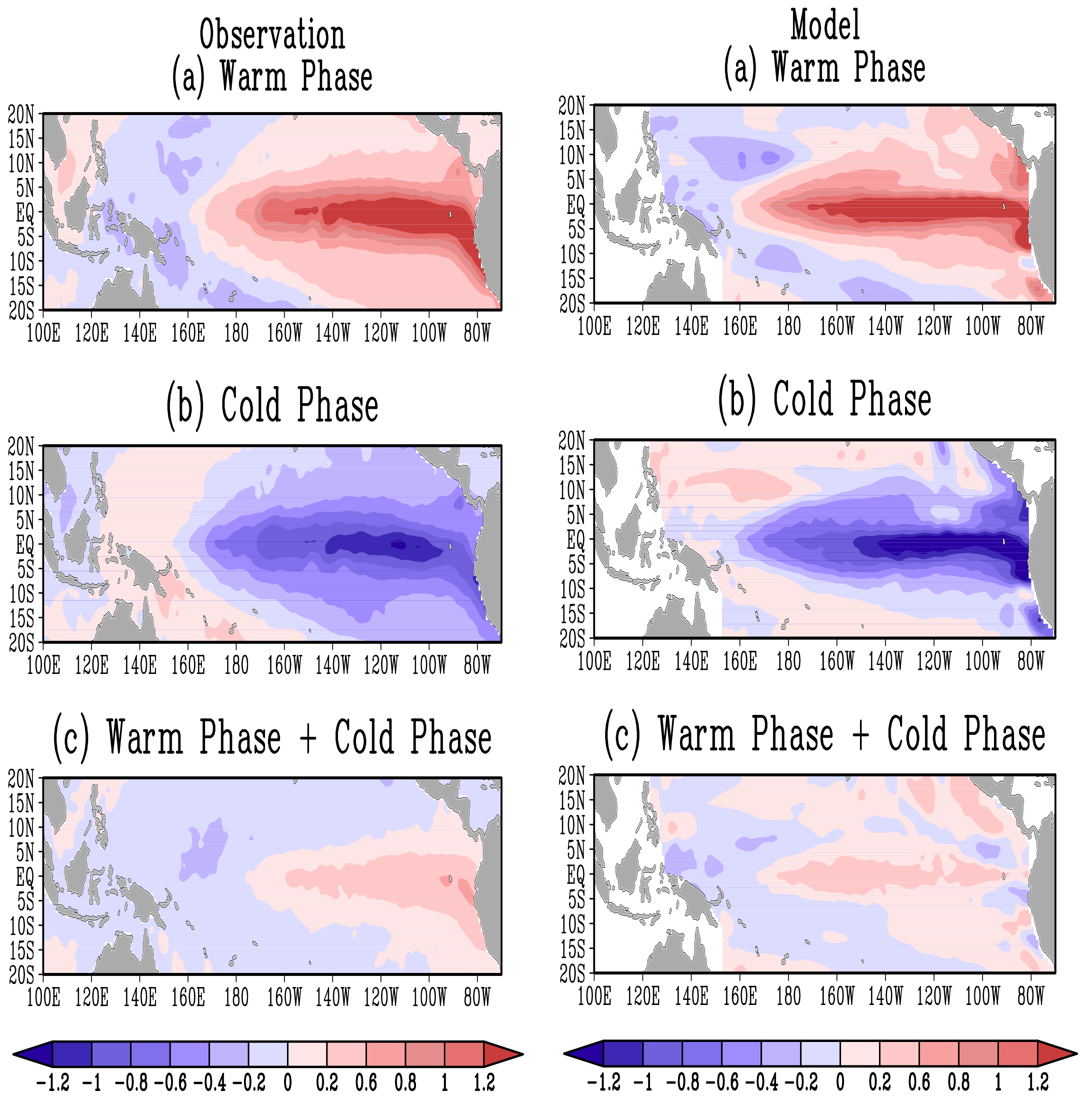

FIG. 3. ENSO SST anomalies—warm phase (a), cold phase (b), and residual (warm phase + cold phase) (c) in the observations (left panels) and in the forced ocean GCM experiment (right panels). A 0.5 $^{\circ}$C threshold value for the monthly SST anomaly was used for obtaining the warm phase and cold phase composites. The same threshold value was used for both the model simulations and the observations.

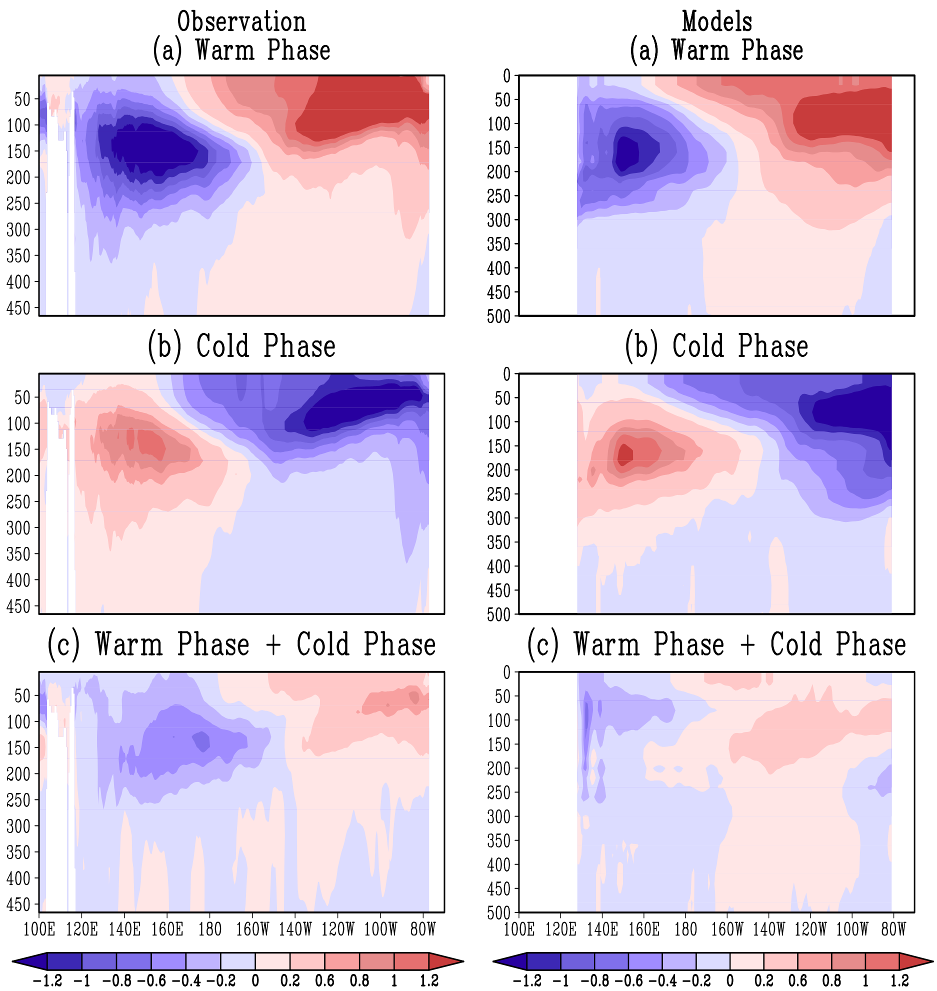

FIG. 4: ENSO temperature anomalies in the equatorial upper ocean (5°S-5°N)—warm phase (a), cold phase (b), and residual (warm phase + cold phase) from observations (d) (left panels) and from the forced ocean GCM experiment (right panels). A 0.5 °C threshold value for the monthly SST anomaly was used for obtaining the warm phase and cold phase composites. The same threshold value was used for both the model simulations and the observations.

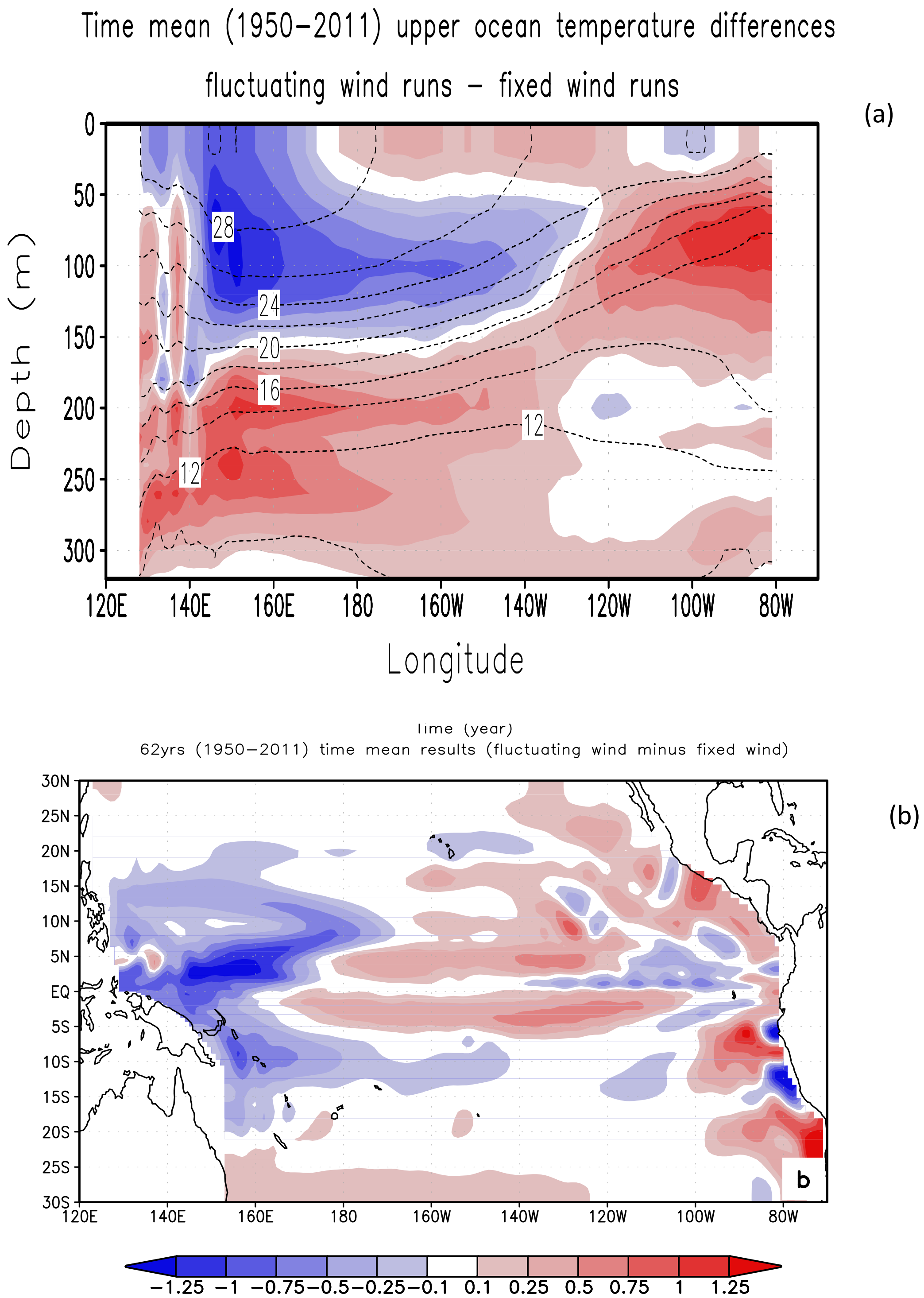

FIG. 5. (a) Time-mean temperature differences in the equatorial upper ocean (5^{o}S-5^{o}N) between the run with ENSO in the surface forcing and the run without ENSO in the surface forcing. (Dashed contour lines are the time-mean temperature fro the run without ENSO). (b) The corresponding SST differences.

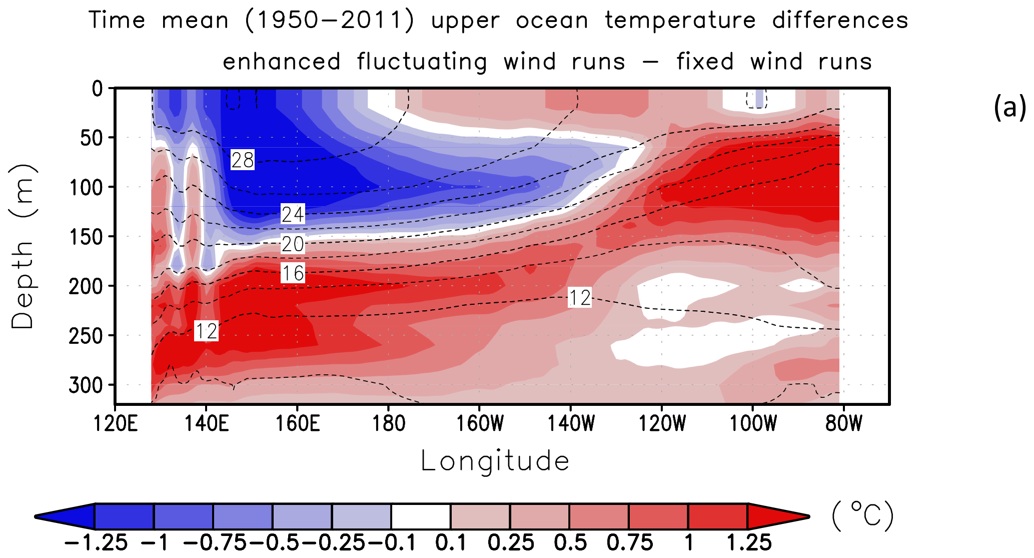

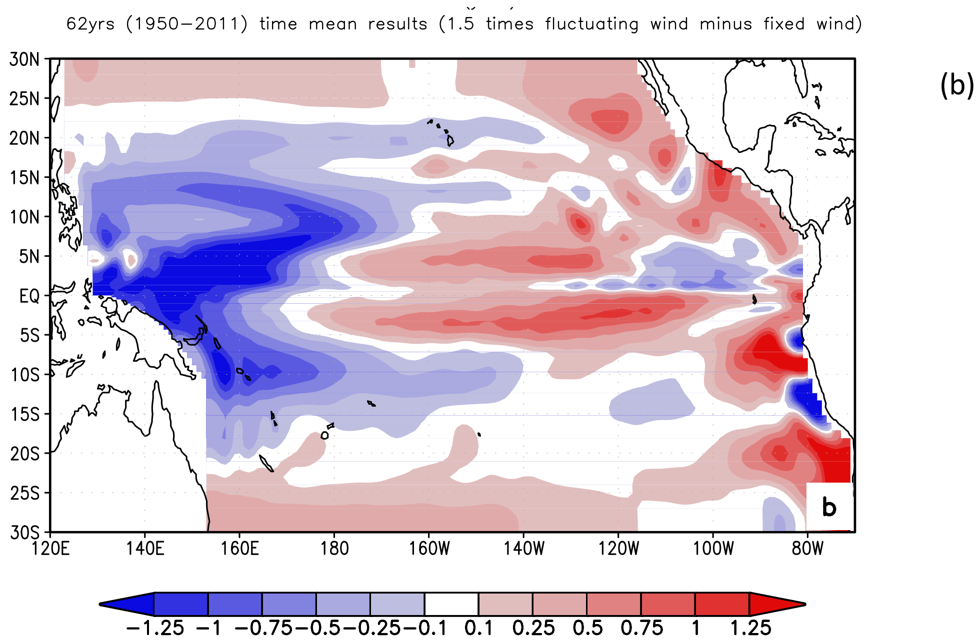

FIG. 6. Same as in Fig. 5 except the magnitude of ENSO fluctuations in the surface forcing for the forced run is enhanced by 50% (measured by standard deviation). The standard deviation of the resulting Nino3 SST with the enhanced ENSO fluctuation in the surface forcing is enhanced by about the same amount (from 0.79 ^{o}C to 1.15 ^{o}C).

(a)

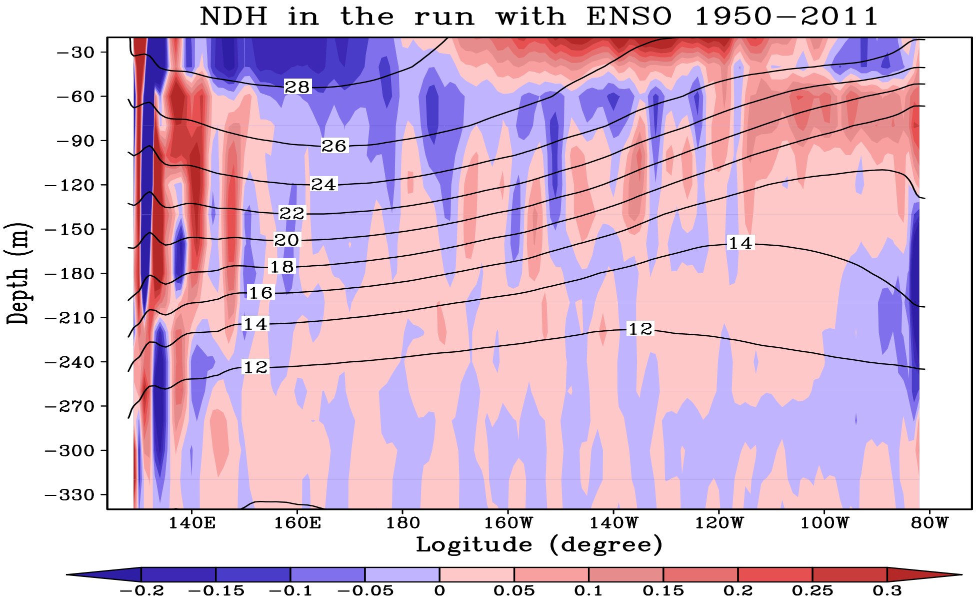

(b)

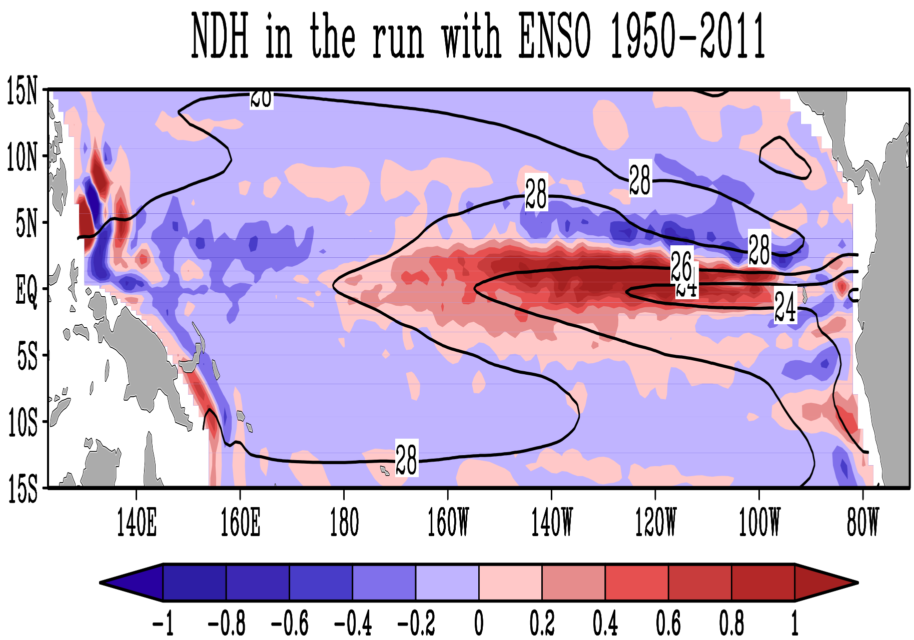

FIG. 7: Distribution of Nonlinear Dynamics Heating (NDH) in the run with ENSO for the equatorial upper ocean (5°S-5°N) as a function of longitude and depth (a) and for the surface layer of the tropical Pacific as a function of latitude and longitude (b). The contours are the corresponding time mean upper ocean temperature (a) and SST (b).

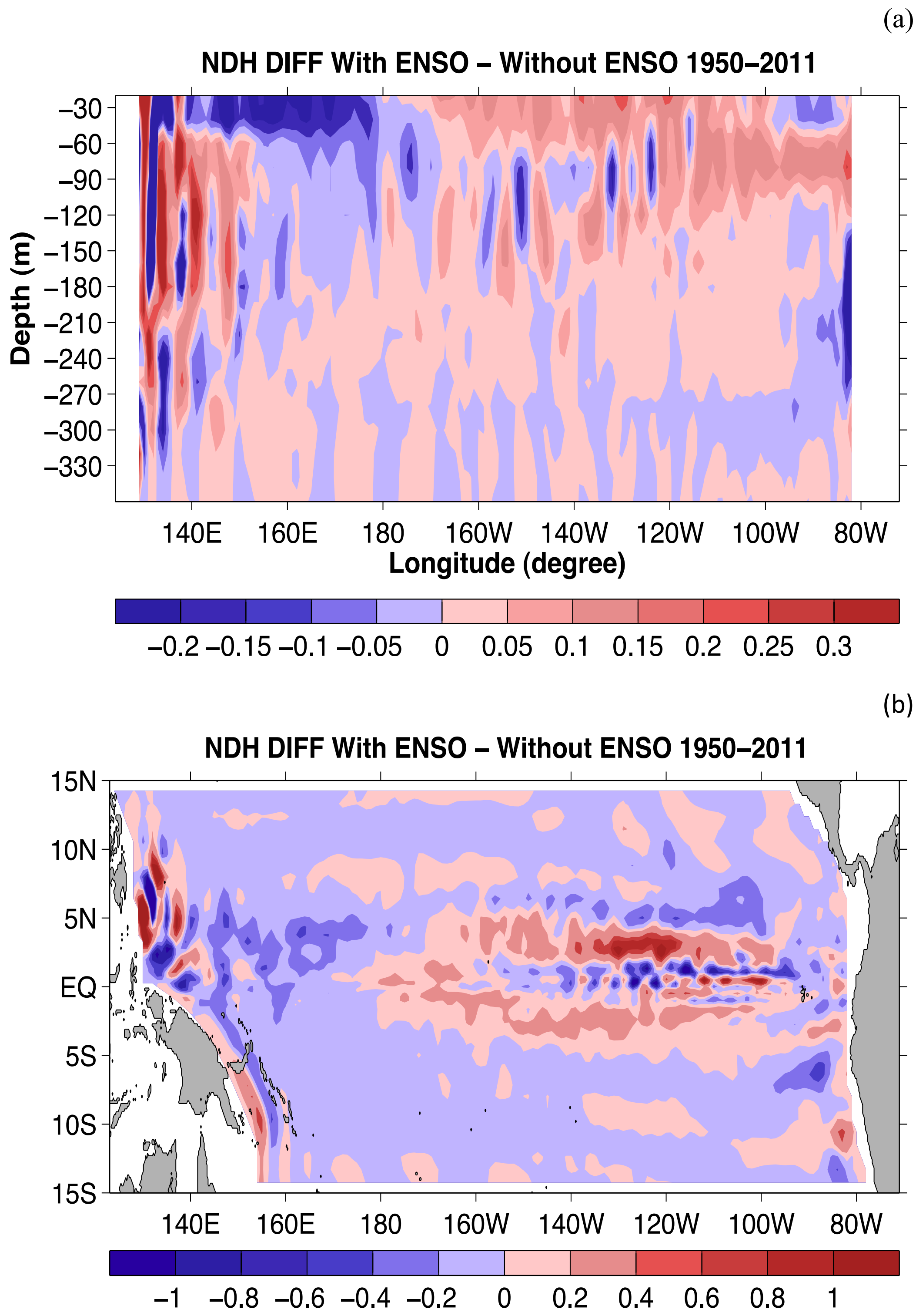

FIG. 8: Same as in Fig. 7 except that they are the differences between the run with ENSO and the run without ENSO.

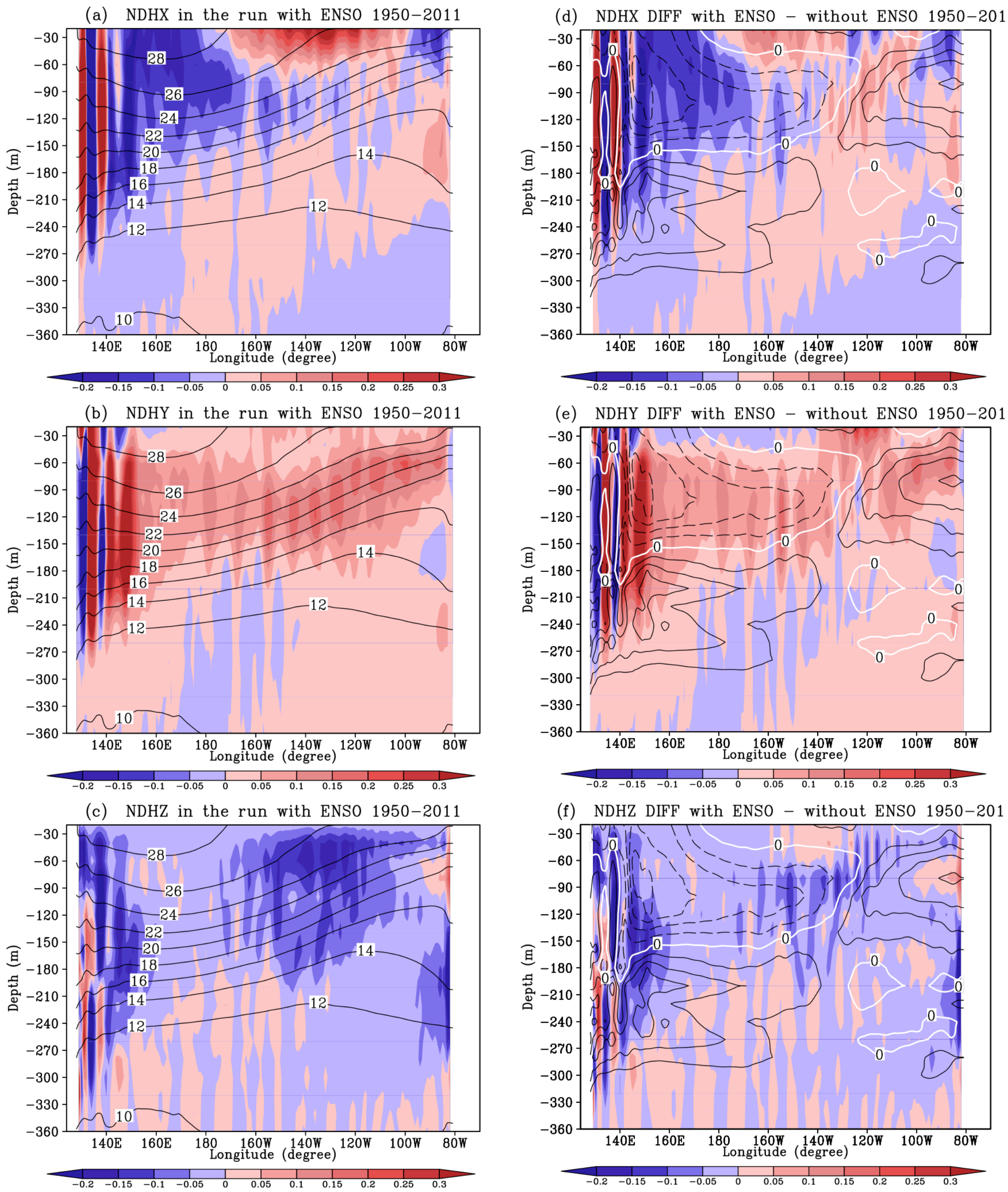

FIG. 9: The zonal (a), meridional (b), and vertical (c) components of the Nonlinear Dynamics Heating (NDH) in the equatorial upper ocean (5^{o}S-5^{o}N) as a function of longitude and depth in the run with ENSO (left three panels). (Contours in these figures (a, b, c) are the corresponding time-mean upper ocean temperature). The right three panels (d, e, f) show respectively the same quantities as in left three panels, but with the corresponding term in the run without ENSO removed. (Contours in the figures (d, e, f) are the differences in the time-mean upper ocean temperature between the run with ENSO and the run without ENSO).

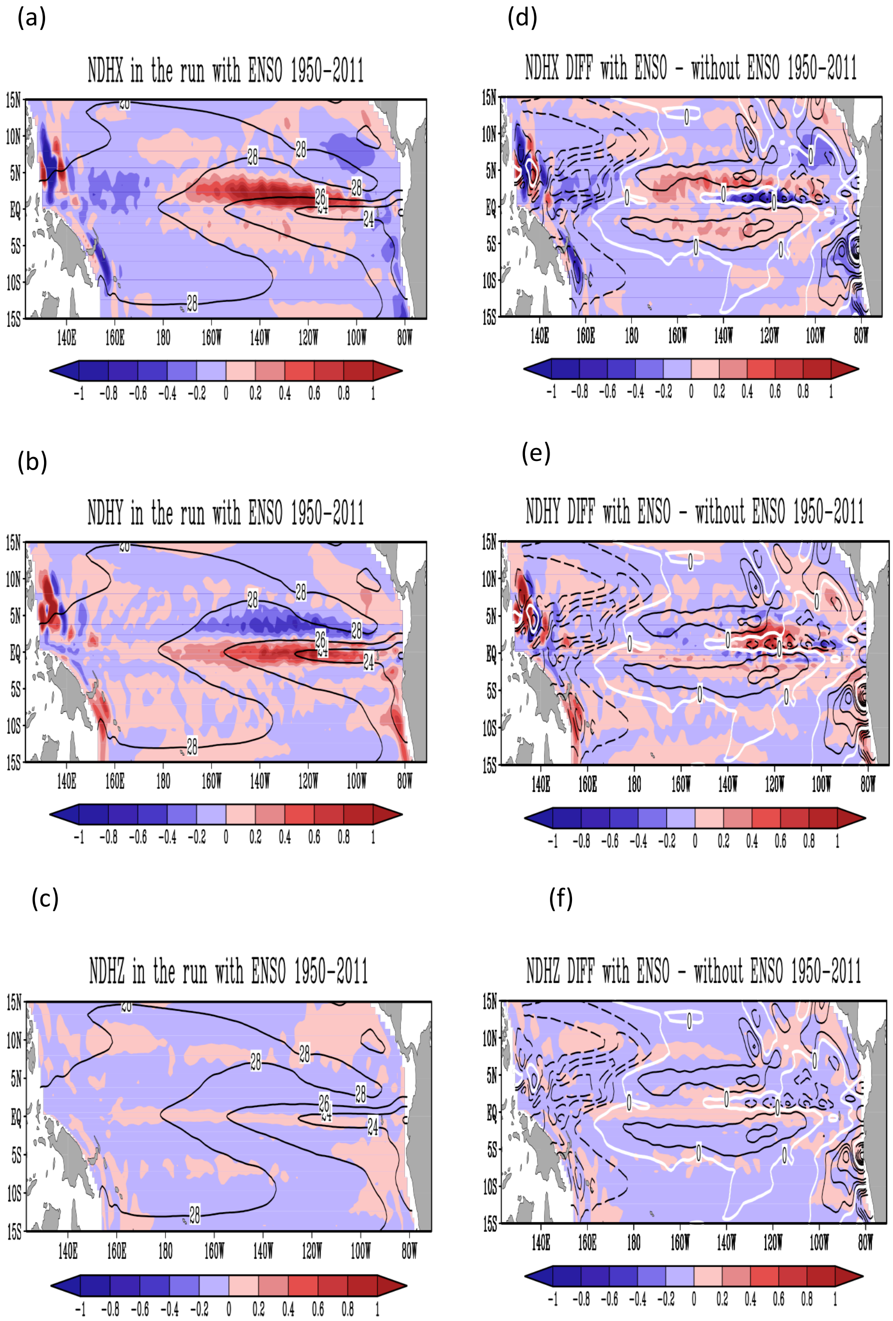

FIG. 10: The zonal (a), meridional (b), and vertical (c) components of the Nonlinear Dynamics Heating (NDH) as a function of longitude and latitude for the surface layer in the run with ENSO (left three panels). (Contours in the figures (a, b, c) are the corresponding time-mean SST). The right three panels (d, e, f) show respectively the same quantity as in the left three panels, but with the corresponding term in the run without ENSO removed. (Contours in the figures (d, e, f) are the differences in the time-mean SST between the run with ENSO and the run without ENSO.)